REVISTA CUBANA DE CIENCIAS BIOLÓGICAS
http://www.rccb.uh.cu

ARTÍCULO ORIGINAL

Structure-activity relationship of the inhibition of M1-aminopeptidases from *Escherichia coli* (ePepN) and *Plasmodium falciparum* (PfA-M1) by bestatin-derived peptidomimetics

Relación estructura-actividad de la inhibición de aminopeptidasas M1 de Escherichia coli *(ePepN) y* Plasmodium falciparum (*PfA-M1) por peptidomiméticos derivados de la bestatina*

Ana C. Varela[1], Idalia Pérez[1], German De Armas[1], Yanira Méndez[2], Maikel Izquierdo[1], Maday Alonso del Rivero[1], Daniel G. Rivera[2], Jorge González-Bacerio[1,3]*

[1] Center for Protein Studies, Faculty of Biology, University of Havana, Cuba.
[2] Center for Natural Products Research, Faculty of Chemistry, University of Havana, Cuba.
[3] Department of Biochemistry, Faculty of Biology, University of Havana, Cuba.

* Autor para correspondencia: jogoba@fbio.uh.cu

Recibido: 2019-04-10

Aceptado: 2019-06-04

ABSTRACT

The enzymes ePepN and PfA-M1 are two M1 alanyl-aminopeptidases which are targets in the potential treatment of microbial infections and malaria, respectively. The classical inhibitor of M1-aminopeptidases is bestatin. The synthetic bestatin-derived peptidomimetic KBE009 was previously identified as a PfA-M1 inhibitor with *in vitro* antimalarial activity. The objective of this work was to test a synthetic library of 10 bestatin (KBE009)-derived peptidomimetics in the inhibition of recombinant ePepN (rePepN) and PfA-M1 (rPfA-M1), and to study the resultant structure-activity relationship. In the first place, the main kinetic characteristics of rePepN and of the inhibition of both enzymes by bestatin were assessed. The same rePepN activity at pH 7.0 and 8.0, as well as a K_M = 72 µM toward the Leu-*p*-nitroanilide substrate were determined. A 5-min preincubation between bestatin and rePepN is enough to establish the inhibition equilibrium and bestatin is a non-competitive inhibitor of the enzyme with a K_i = 2.31 µM. On the other hand, for rPfA-M1 a 15-min preincubation time is enough, the K_i of bestatin is 1.29 µM and this inhibitor is competitive. Although none compound is a potent inhibitor, the structural characteristics of the bestatin (KBE009)-derived peptidomimetics that are favorable for the inhibition are: the central isopropyl and terminal 3-phenylpropyl groups in the branch (for both aminopeptidases), the central isopropyl and terminal cyclohexyl groups (for rePepN), and the central 2-furyl and terminal benzyl groups (for rPfA-M1). The compound KBE053, as representative of this series, is an uncompetitive inhibitor of rePepN with a K_i = 10.13 µM. This knowledge could contribute to the design of novel ePepN and PfA-M1 inhibitors.

Keywords: inhibition mode, KBE009, kinetic characterization, structure-activity relationship

RESUMEN

Las enzimas ePepN y PfA-M1 son dos alanil-aminopeptidasas M1 que son blancos en el tratamiento potencial de infecciones microbianas y la malaria, respectivamente. El inhibidor clásico de las aminopeptidasas M1 es la bestatina. El peptidomimético sintético derivado de la bestatina KBE009 fue identificado previamente como un inhibidor de PfA-M1 con actividad antimalárica in vitro*. El objetivo de este trabajo fue evaluar una biblioteca sintética de 10 peptidomiméticos derivados de la bestatina (KBE009) en la inhibición de ePepN y PfA-M1 recombinantes (ePepNr y PfA-M1r), y estudiar la relación estructura-actividad resultante. En primer lugar, se determinaron las principales características cinéticas de ePepNr y de la inhibición de ambas enzimas por la bestatina. Se determinó la misma actividad de ePepNr a pH 7,0 y 8,0, así como una K_M = 72 µM frente al sustrato Leu-p-nitroanilida. Una preincubación de 5 min entre la bestatina y ePepNr es suficiente para establecer el equilibrio de inhibición, y la bestatina es un inhibidor no competitivo de la enzima con una K_i = 2,31 µM . Por otra parte, para PfA-M1r es suficiente un tiempo de preincubación de 15 min, la K_i de la bestatina es 1,29 µM y este inhibidor es competitivo. Aunque ningún compuesto es un inhibidor potente, las características estructurales de los peptidomiméticos derivados de la bestatina (KBE009) que son favorables para la inhibición son: los grupos central isopropilo y terminal 3 -fenilpropilo en la ramificación (para ambas aminopeptidasas), los grupos central isopropilo y terminal ciclohexil (para ePepNr), y los grupos central 2-furilo y terminal bencilo (para PfA-M1r). El compuesto KBE053, como representante de esta serie, es un inhibidor incompetitivo de ePepNr con una K_i = 10,13 µM . Este conocimiento pudiera contribuir al diseño de nuevos inhibidores de ePepN y PfA-M1.*

Palabras clave: *caracterización cinética, KBE009, modo de inhibición, relación estructura-actividad*

INTRODUCTION

The increasing of bacterial resistance to conventional antibiotics has become a worldwide health problem. The development of novel antibacterial drugs, their irrational and indiscriminate use and the evolutionary pressure exerted by the therapeutic use, have favored the increasing of resistant strains (Wilke, 2010; Pathak *et al*., 2012). For this reason, the development of novel antimicrobial agents, directed against novel molecular targets, is a priority (Silver, 2011; Scholz *et al*., 2012).

Malaria is the main human parasitic disease in tropical regions (Greenwood *et al*., 2005) and its more lethal etiologic agent is the protozoon *Plasmodium falciparum*, William H. Welch 1897 (Apicomplexa: Aconoidasida: Haemosporida: Plasmodiidae), responsible of almost half million of deaths annually in all the world (WHO, 2017). The spread parasite resistance to traditional drugs (Turschner and Efferth, 2009) and the absence of an effective vaccine against the disease (Doolan *et al*., 2014) impose the search for novel therapeutic agents.

Proteolysis is a crucial event for bacterial growth and development (Kaman *et al*., 2014). In addition to this essential physiological role, pathogen bacteria segregate proteases as virulent factors that act over host proteins and tissues (Madigan *et al*., 2014). Neutral metallo-aminopeptidases (APs) are included in both processes. Therefore, inhibition of these enzymes could block the growth, diminish the virulence and increase the susceptibility toward antimicrobial agents (Madigan *et al*., 2014).

Host hemoglobin breakdown is an essential event for the development of *P. falciparum* during its clinically relevant erythrocytic stages (Liu *et al*., 2006). This process has been identified as a target for the search for antimalarials (Yeh and Altman, 2006) and involves redundant endoproteases belonging to different mechanistic classes (Omara-Opyene *et al*., 2004), as well as neutral metallo-APs (Dalal and Klemba, 2007).

Metallo-proteases are the most diverse mechanistic class of these hydrolases and contain in the active site at least a divalent metallic cation with catalytic function (Barret *et al*., 2003). Among these enzymes are included APs, which hydrolyze the N-terminal peptide bonds of polypeptide chains. Neutral metallo-APs, denomination based on the substrate specificity, are a distinctive group that develop crucial biological functions in different organisms (Albiston *et al*., 2004; Luan and Xu, 2007; Noble and Roques, 2007), including their essential role in the life cycles of different parasites. For this reason, such peptidases are recognized

as targets in relevant human parasitic diseases (Morty and Morehead, 2002; Cadavid-Restrepo *et al*., 2011). That is the case of PfA-M1, an alanyl-AP belonging to the M1 family (APN) of metallo-proteases that is present in *P. falciparum* and constitutes a promising target against malaria (Florent *et al*., 1998; Harbut *et al*., 2011).

Native PfA-M1 (nPfA-M1) is a monomeric enzyme of 1,085 aminoacid residues and 126 kDa as primary protein. Its gene is expressed in the erythrocytic stage of the parasite life cycle as three active and soluble processed proteins of 120, 96 and 68 kDa (Florent *et al*., 1998; Allary *et al*., 2002; Azimzadeh *et al*., 2010). This AP contains a Zn^{2+} ion in the active site (McGowan *et al*., 2009) and it is specific for peptides with basic and hydrophobic residues in the N-terminal (Allary *et al*., 2002; Dalal *et al*., 2012; Poreba *et al*., 2012). This essential enzyme (Dalal and Klemba, 2007) participates in the hydrolysis of dipeptides derived from the hemoglobin breakdown, among other functions (Gavigan *et al*., 2001; Allary *et al*., 2002; Dalal and Klemba, 2007; Harbut *et al*., 2011; Ragheb *et al*., 2011). Some PfA-M1 inhibitors previously described have *in vitro* antimalarial activity at micromolar or submicromolar concentrations, as well as *in vivo* in murine models (Flipo *et al*., 2007a; Skinner-Adams *et al*., 2007, 2012; Harbut *et al*., 2011; Velmourougane *et al*., 2011). For this reason, identification of PfA-M1 inhibitors is a priority in this research area. In our group, a recombinant variant of PfA-M1 (rPfA-M1) is available (González-Bacerio *et al*., 2014a).

Another AP, among the most studied with these aims, is the APN from the gram-negative bacterium *Escherichia coli* (ePepN). This enzyme contains a catalytic Zn^{2+} ion in the active site. It shows the highest ATP-independent AP activity in *E. coli* and is involved in the last stages of the protein degradation pathway in the bacterial cytosol (Chandu and Nandi, 2003; Chandu *et al*., 2003). For these reasons, this enzyme develops relevant functions in the cellular maintaining, growth and development. The AP ePepN is highly conserved among prokaryotes, including pathogen bacteria (Chandu *et al*., 2003). The previous elements, together with its easy obtainment by recombinant way (Addlagatta *et al*., 2006), determine that this AP is a good model for the fast identification of inhibitors of APNs from pathogen microorganisms (Chandu *et al*., 2003). Therefore, ePepN is an attractive target for use in the search for natural and synthetic inhibitors, and for studying the structure-activity relationship of identified inhibitors. In our group, an ePepN recombinant variant (rePepN) is available (Méndez *et al*., 2019).

The design of synthetic compounds for the APN inhibition is based in the presence of Zn^{2+} ion in the active site and the S1 and S1' enzyme subsites. For example, the PfA-M1 S1 subsite is composed of the residues Q^{317}, E^{319}, A^{320}, V^{459}, M^{462}, E^{572}, Y^{575} and M^{1034}; and the S1' pocket is formed by R^{489}, T^{492}, V^{493} and V^{523} (McGowan *et al*., 2009; Velmourougane *et al*., 2011; Drinkwater *et al*., 2015). As in ePepN (Addlagatta *et al*., 2008), the PfA-M1 S1 pocket has the shape of a cylinder with hydrophobic walls that accommodate the non-polar side chains of some P1 residues. At the end of this pocket are polar residues, as E^{572} (McGowan *et al*., 2009). It has been proposed that the long basic chains of arginine and lysine in the P1 site of peptide ligands establish hydrophobic interactions with the S1 subsite wall, while the positive charge ends of these residues interact by hydrogen bonds with E^{572} (Dalal *et al*., 2013; Kannan Sivaraman *et al*., 2013; Rosati *et al*., 2017). Therefore, the synthetic APN inhibitors have substituents (in P1 hydrophobic or long basic; in P1' hydrophobic or long with polar ends; Dalal *et al*., 2012) destined to recognize the S1 and S1' pockets, and specific functional groups to coordinate the Zn^{2+} (Xu and Li, 2005; Mucha *et al*., 2010).

Neutral metallo-APs from M1 and M17 families are inhibited by bestatin (Burley *et al*., 1991; Scornik and Botbol, 2001; Addlagatta *et al*., 2006), a natural pseudopeptide, transition state analog of the catalytic mechanism of these enzymes (Umezawa *et al*., 1976). This compound, that mimics the structure of the Phe-Leu dipeptide, is considered as a slow-binding competitive reversible inhibitor (Scornik and Botbol, 2001). The inhibition constant (K_i) of bestatin toward ePepN is in units of micromolar (Fournié-Zaluski *et al.*, 2009) and toward PfA-M1 is in the 3.8-0.12 µM range (McGowan *et al*., 2009; Ragheb *et al*., 2011; Velmourougane *et al*., 2011; Skinner-Adams *et al*., 2012). For this reason, such inhibitor has an intermediate potency between classical and tight-binding inhibition.

In addition to inhibiting APNs, this compound inhibits the growth of some pathogenic bacteria, as *Porphyromonas gingivalis* (Labbé *et al*., 2001) and *Helicobacter pylori* (Dong *et al*., 2005; Modak *et al*., 2016). This compound also inhibits the *in vitro* growth of *P. falciparum* with half maximal inhibitory concentration

(IC_{50}) values from tens to units of µM (Nankya-Kitaka *et al*., 1998; Flipo *et al*., 2003; Skinner-Adams *et al*., 2007). A major disadvantage of bestatin for the therapy of bacterial infections and malaria is its low selectivity for the inhibition of neutral and basic APs, since it also inhibits these human enzymes (Scornik and Botbol, 2001; Drinkwater *et al*., 2017). Despite this, its chemical structure can be used as a basis to design compounds that could be used for the treatment of bacterial infections and malaria.

This pseudopeptide has been used as a model inhibitor to study the structure-function relationship of this type of APs, including ePepN and PfA-M1 (Addlagatta *et al*., 2006; McGowan *et al*., 2009; Chen *et al*., 2012; Wong *et al*., 2012). The main interactions between bestatin and ePepN and PfA-M1 active site, determined by X-ray crystallography, are the following: (1) The hydroxyl and carbonyl groups of the phenylalanine-like residue in bestatin coordinate the Zn^{2+} ion. (2) The benzyl and isobutyl substituents of the inhibitor establish hydrophobic interactions with the side chains of several residues from the active site's S1 and S1' subsites, respectively. (3) The free amino group of bestatin establishes hydrogen bonds with the side chains of two active site's glutamates (Addlagatta *et al*., 2006; McGowan *et al*., 2009).

We previously identified KBE009, a synthetic bestatin-based peptidomimetic which is a submicromolar rPfA-M1 inhibitor (K_i = 0.4 µM) and an *in vitro* antimalarial compound as potent as bestatin (IC_{50} = 18 µM) (González-Bacerio *et al*., 2017). The compound KBE009 inhibits the M1-type AP activity in isolated live parasites with a potency similar to that of the antimalarial activity (IC_{50} = 82 µM), strongly suggesting that the antimalarial effect is directly related to the inhibition of the endogenous PfA-M1. Docking simulations indicate that this compound binds PfA-M1 without Zn^{2+} coordination, establishing mainly hydrophobic interactions and showing a remarkable shape complementarily with the active site of the enzyme (González-Bacerio *et al*., 2017). To study the structure-activity relationship of compounds similar to KBE009, in this work we assess the inhibition of APNs ePepN and PfA-M1 by a library of 10 synthetic bestatin (KBE009)-derived peptidomimetics (including KBE009). These compounds have different structural elements with potentialities for the interaction with the S1 and S1' subsites of both enzymes, both in steric complementarily and in physical-chemical recognition.

MATERIALS AND METHODS

Enzymes, substrate, bestatin and bestatin (KBE009)-derived peptidomimetics

The enzymes rePepN and rPfA-M1 were obtained in the Center for Protein Studies, Faculty of Biology, University of Havana, where they are produced routinely (González-Bacerio *et al*., 2014a; Méndez *et al*., 2019). Since both recombinant enzymes were obtained with a purity >90 % (González-Bacerio *et al*., 2014a; Méndez *et al*., 2019), we report enzyme concentration in molarity. The chromogenic peptidic substrate Leu-*p*-nitroanilide (Leu-*p*NA) and the inhibitor bestatin were obtained in Bachem (Sweden). The bestatin (KBE009)-derived peptidomimetics were synthesized in the Center for Natural Products Studies, Faculty of Chemistry, University of Havana (Méndez *et al*., 2014). These are low-molecular-weight compounds that have different substituents with distinct hydrophobicities and sizes. They are based on the bestatin's Phe-Leu scaffold N-alkylated in the amide nitrogen. This central chain (absent in the bestatin structure) has two variable groups: one in the branching in the first carbon after amide nitrogen (neither, 2-furyl, isopropyl or *p*-methoxyphenyl), and the other terminal after a second amide bond (benzyl, cyclohexyl or 3-phenylpropyl). The objective is to expand contacts with the active sites through these hydrophobic substituents.

Aminopeptidase activity assays for rePepN and rPfA-M1

The AP enzymatic activity (EA) was determined by a continuous kinetic method (Tieku and Hooper, 1992). The chromogenic substrate Leu-*p*NA 75 µM, for rePepN, and 300 µM, for rPfA-M1, was used (~1 apparent Michaelis-Menten's constant ($appK_M$); dissolved in DMSO; 2 µLfor the microplate assay and 10 µL for the cuvette assay) and the increase of the absorbance at 405 nm (due to the liberation of the *p*NA chromogen) was recorded in function of time for 3 min, making measurements each 15 s. The determinations were done at 25ºC, as in 96-well microplates (200 µL final volume), using a microplate spectrophotometer (Multiscan FC, Thermo Scientific, USA), as in a cuvette of 1 cm of path length (1 mL final volume), using a kinetic spectrophotometer (UV-1800 Shimadzu, UV Spectrophotometer, Japan). The buffer 50 mM Tris-HCl pH 8.0, for rePepN, and pH 7.2, for rPfA-M1,

was used, as well as concentrations of rePepN (7.5 x 10^{-8} M) or rPfA-M1 (5.3 x 10^{-8} M) linearly related with the initial velocities (v_0). The final DMSO concentration in the assays was not higher than 2 % (v/v). Only the linear portions of the progress curves, corresponding to substrate consumption lower than 5 %, were used to measure the reaction rates. The slopes with $R^2 < 0.98$ were not considered. The slope values of the reaction progress curves (ΔAbs/Δt) were taken as values of v_0. The assays were performed in quadruplicate.

Comparison between the rePepN aminopeptidase activities at pH 7.0 and 8.0

Aminopeptidase activity assays were performed at pH 7.0 and 8.0, using the Leu-*p*NA substrate at 300 µM (~ 4 appK_M). The remaining experimental conditions were as described.

Determination of the rePepN apparent K_M value toward the Leu-*p*NA substrate

To determine the rePepN appK_M, AP activity assays were performed at seven concentrations of the Leu-*p*NA substrate (18.75-1,200 µM), prepared by double serial dilutions in DMSO. Since the enzymatic preparation used in this work does not contain rePepN purified until total homogeneity (Méndez *et al*., 2019), K_M is reported as an apparent value. The appK_M was calculated by fitting the function of the Michaelis-Menten's rectangular hyperbole (Copeland, 2000) to the experimental data. For this, the OriginPro 8 SR0 software was used (version 8.0724 (B724); OriginLab Corporation [http://www.OriginLab.com]).

Aminopeptidase activity inhibition assays for rePepN and rPfA-M1

The rePepN or rPfA-M1 enzymes were preincubated with 10 µL (for the cuvette assay) or 2 µL (for the microplate assay) of bestatin or the compounds (dissolved in DMSO), at 25ºC for 15 min. Subsequently, the substrate Leu-*p*NA at 75 µM, for rePepN, and 300 µM, for rPfA-M1 (~1 appK_M), was added and the AP activity assays were performed. The control was prepared by pre-incubation of the enzymes with the same volume of DMSO in the previous conditions. The residual activity (v_i/v_0) was defined as the ratio between the reaction rate in the presence of the compound and the reaction rate corresponding to the control.

Determination of the time necessary to reach the inhibition equilibrium

Inhibition assays with rePepN or rPfA-M1 and bestatin were performed by pre-incubation of the enzymes with the inhibitor during 5, 10, 15, 30 and 45 min.

Determination of the inhibition mode

Assays of AP EA with rePepN in the presence of 0, 4 and 10 µM bestatin or 0, 12.5, 25 and 40 µM KBE053, and rPfA-M1 in the presence of 0, 0.78, 1.56 and 3.12 µM bestatin, were performed. For each inhibitor concentration, after pre-incubation for 15 min, the substrate Leu-*p*NA was added at different concentrations, spanning the range 18.75-1,200 µ M in the assay. In the absence of inhibitor, the enzymes were preincubated with the same DMSO volume. The experimental data were transformed and the Lineweaver-Burk double reciprocal plots were constructed. The transformed experimental data were analyzed by a simple linear fitting using the software Microsoft Office Excel 2007™ (Microsoft Corporation; USA; [https://www.microsoft.com/]). The inhibition type was determined graphically from the lines of the double reciprocal plots (Copeland, 2000).

Determination of K_i

For bestatin toward rePepN, K_i was determined by Dixon plot (1/apparent maximum velocity (appv_{max}) *vs*. bestatin concentration) to determine the -αK_i value, and the other secondary plot (slope Lineweaver–Burk plots vs. bestatin concentration), to determine the -K_i value (Copeland, 2000). For bestatin toward rPfA-M1, K_i was determined by Dixon plot ($1/v_0$ *vs*. bestatin concentration) at two different substrate concentrations. For KBE053 toward rePepN, K_i was determined by Dixon plot (1/appv_{max} *vs*. KBE053 concentration) to determine the -αK_i value, assuming that α can be considered as zero in uncompetitive inhibition (Copeland, 2000).

Dose-response studies for the inhibition of the rePepN and rPfA-M1 enzymes

The inhibition assays of the rePepN and rPfA-M1's EA with bestatin (for rPfA-M1) and the bestatin (KBE009)-derived peptidomimetics (for both enzymes) were performed. Different concentrations of each compound were used (prepared in DMSO by double serial dilutions) spanning the range 0.781-100 µM

(concentrations in the assay). When the IC_{50} value was not reached in this range, lower or higher inhibitor concentrations were tested. The IC_{50} values were calculated from the dose-response curves (residual activity *vs*. inhibitor concentration in logarithmic scale) by the nonlinear fit of the logistic function to the experimental data, using OriginPro 8 SR0 software (version 8.0724 (B724); OriginLab Corporation [http://www.OriginLab.com]) with default parameters. The logistic function is: $v_i/v_0 = 1 / (1 + [I] / IC_{50})$, where [I]: inhibitor concentration in the assay (Copeland, 2000). All assays were performed at least in triplicate.

Statistical analyses

Normal distribution and homogeneity of variances of the experimental data were verified by the Kolmogorov-Smirnov and the Bartlett test, respectively (Snedecor and Cochran, 1989). Afterward, an analysis of variance of simple classification was carried out. The means were compared by the Tukey HSD test (Tukey, 1949). A level of signification of 0.05 was used. To perform these analyses, the software Statistica (version 8.0; StatSoft Inc. [http://www.statsoft.com]) was used.

RESULTS

Partial kinetic characterization of rePepN aminopeptidase and the inhibition of rePepN and rPfA-M1 by bestatin

Firstly the main kinetic characteristics of rePepN, that is necessary to know for the inhibitors identification, were assessed. It was confirmed that the activity of this AP toward Leu-*p*NA substrate is the same at pH 7.0 and 8.0 (Fig. 1A). In addition, an $appK_M$ value of 72 µM was obtained (Fig. 1B).

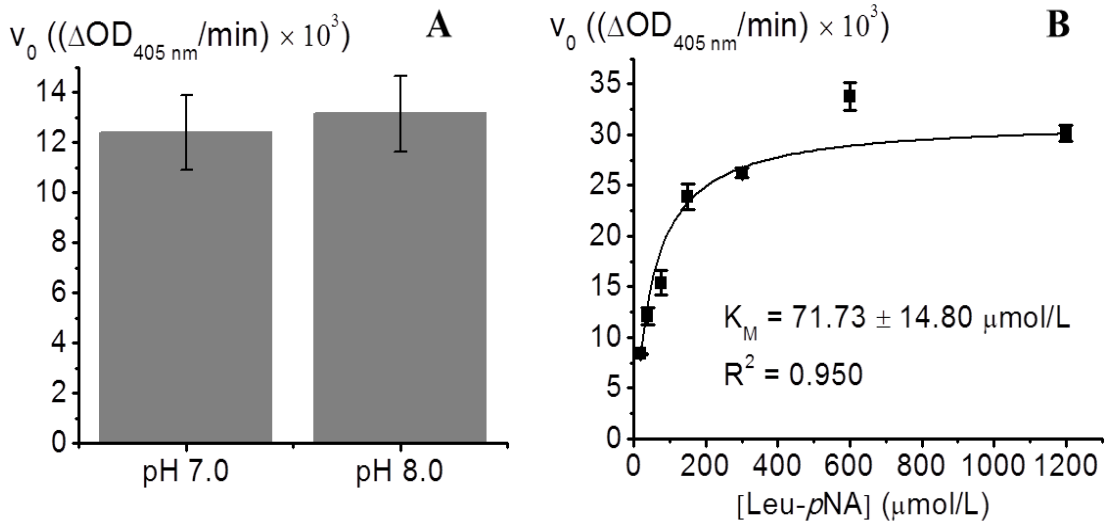

Figure 1. Partial kinetic characterization of rePepN aminopeptidase toward Leu-*p*NA substrate. A) Comparison between the enzymatic activities at pH 7.0 and 8.0. A substrate concentration of 300 µM (~4 $appK_M$) was used. B) Michaelis-Menten's curve. The K_M value is apparent. All data are presented as mean ± standard deviation or standard error (K_M value).

Figura 1. *Caracterización cinética parcial de la aminopeptidasa ePepNr frente al sustrato Leu-pNA. A) Comparación entre las actividades enzimáticas a pH 7,0 y 8,0. Se usó una concentración de sustrato de 300 µM (~4 $K_M$ap). B) Curva de Michaelis-Menten. El valor de K_M es aparente. Todos los datos se presentan como la media ± desviación estándar o error estándar (valor de K_M).*

Afterward, some kinetic characteristics of rePepN inhibition by bestatin were determined. A preincubation time of 5 min between the AP and bestatin is enough to reach the inhibition equilibrium, in the experimental conditions used in this work (Fig. 2A). Bestatin is a non-competitive inhibitor ($\alpha > 1$) or mixed of the enzyme (Fig. 2B), with an α and a K_i value of 3.35 and 2.31 µM, respectively (Fig. 2C and D).

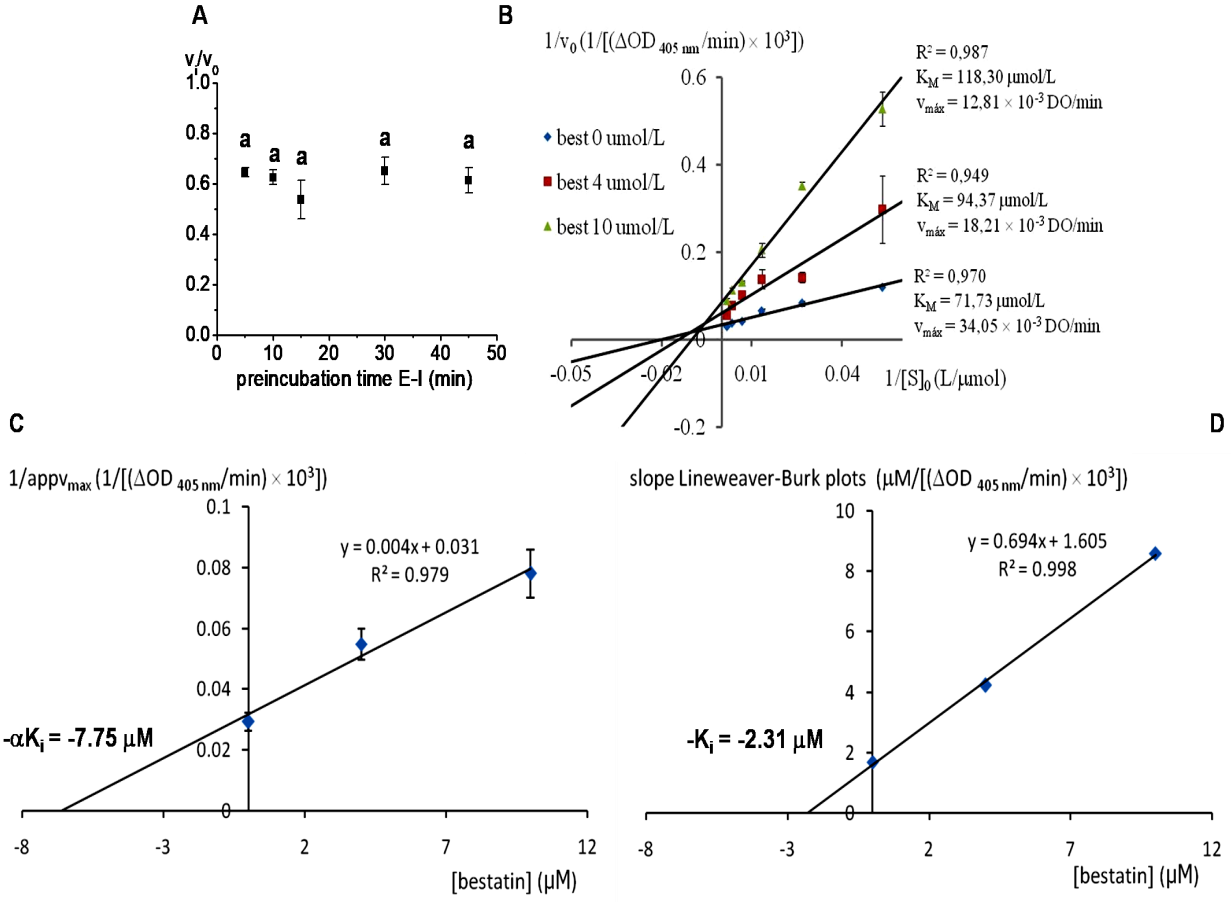

Figure 2. Some kinetic characteristics of rePepN inhibition by bestatin. A) Study of the enzyme-inhibitor preincubation time, necessary to reach the inhibition equilibrium. E: enzyme. I: inhibitor. B) Determination of the inhibition type. K_M and maximum velocity (v_{max}) values are apparent. best: bestatin. C) Dixon plot to determine the $-\alpha K_i$ value (intercept with the abscise axis). D) Secondary plot to determine de $-K_i$ value (intercept with the abscise axis). All data are presented as mean ± standard deviation.

Figura 2. *Algunas características cinéticas de la inhibición de ePepNr por la bestatina. A) Estudio del tiempo de preincubación enzima-inhibidor, necesario para alcanzar el equilibrio de inhibición. E: enzima. I: inhibidor. B) Determinación del tipo de inhibición. Los valores de K_M y velocidad máxima ($v_{máx}$) son aparentes. best: bestatina. C) Ploteo de Dixon para determinar el valor de $-\alpha K_i$ (intercepto con el eje de las abcisas). D) Ploteo secundario para determinar el valor de $-K_i$ (intercepto con el eje de las abcisas). Todos los datos se presentan como la media ± desviación estándar.*

With respect to rPfA-M1, firstly some kinetic features of inhibition by bestatin were assessed. A preincubation time of 15 min between the AP and bestatin is enough to reach the inhibition equilibrium, in the experimental conditions used here (Fig. 3A). An IC_{50} of 1.79 µM for bestatin toward this enzyme and the Leu-*p*NA substrate was determined (Fig. 3B), as well as that this is a competitive inhibitor of rPfA-M1 (Fig. 3C) with a K_i value of 1.29 µM (Fig. 3D).

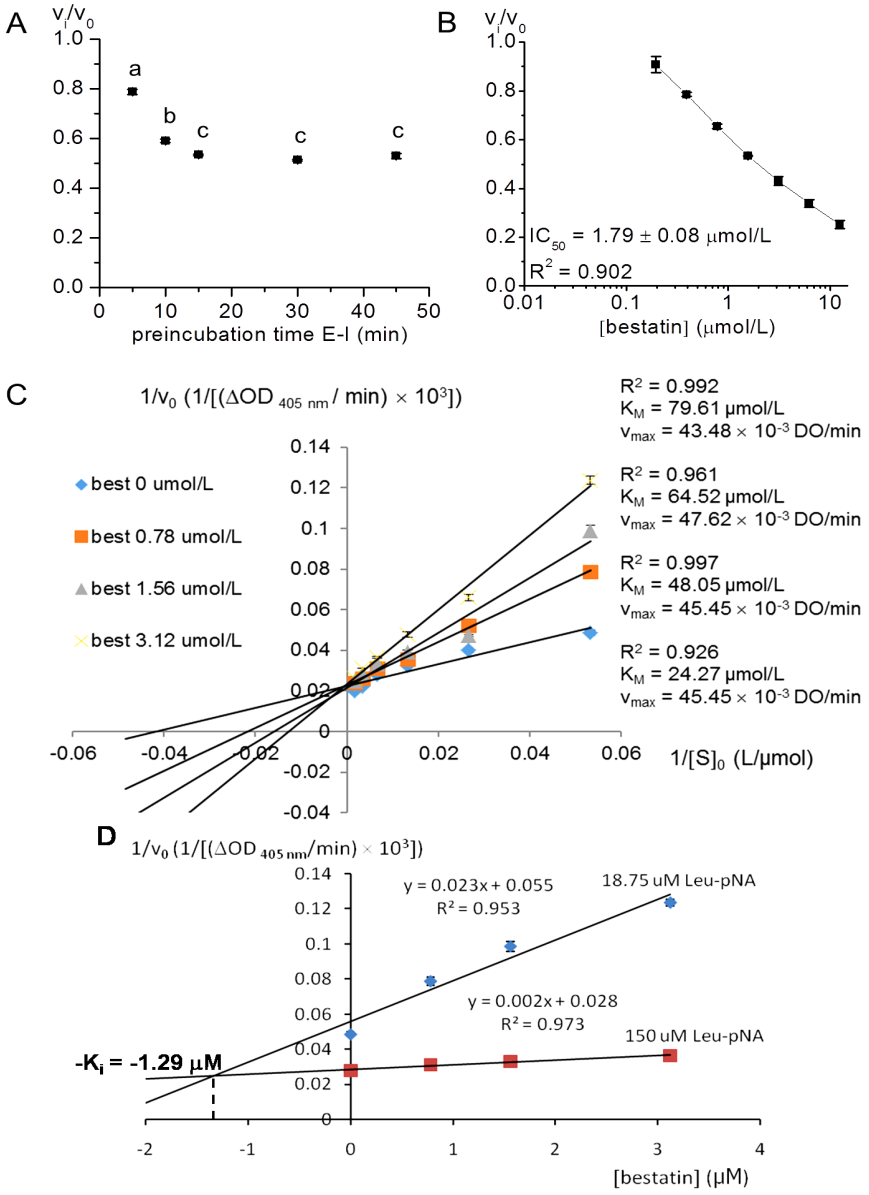

Figure 3. Some kinetic characteristics of rPfA-M1 inhibition by bestatin. A) Study of the enzyme-inhibitor preincubation time, necessary to reach the inhibition equilibrium. E: enzyme. I: inhibitor. B) Dose-response study. Data are presented as means ± standard deviation or standard error (IC_{50} value). C) Determination of the inhibition type. K_M and maximum velocity (v_{max}) values are apparent. best: bestatin. D) Dixon plot to determine the $-K_i$ value (intercept of the two lines). Data are presented as mean ± standard deviation.

Figura 3. *Algunas características cinéticas de la inhibición de PfA-M1r por la bestatina. A) Estudio del tiempo de preincubación enzima -inhibidor, necesario para alcanzar el equilibrio de inhibición. E: enzima. I: inhibidor. B) Estudio dosis-efecto. Los datos se presentan como la media ± desviación estándar o error estándar (valor de IC_{50}). C) Determinación del tipo de inhibición. Los valores de K_M y velocidad máxima ($v_{máx}$) son aparentes. best: bestatina. D) Ploteo de Dixon para determinar el valor de $-K_i$ (intercepto de las dos rectas). Los datos se presentan como la media ± desviación estándar.*

Evaluation of the synthetic bestatin (KBE009)-derived peptidomimetics in the inhibition of rePepN and rPfA-M1 aminopeptidases

The series of 10 synthetic bestatin (KBE009)-derived peptidomimetics was evaluated in the search for possible rePepN inhibitors. Dose-response studies were performed and IC_{50} values were determined.

The 10 compounds were inhibitors of the AP, although with different potency (table 1). The IC_{50} values fluctuate between 26 and 570 µM, approximately. Three peptidomimetics have values higher than 100 µM (KBE045, 049 and 051), and seven in the 10-100 µM range (KBE009, 044, 046, 048, 052, 053 and 054).

Table 1. Inhibition of the rePepN aminopeptidase by the bestatin (KBE009)-derived peptidomimetics

Tabla 1. *Inhibición de la aminopeptidasa ePepNr por los peptidomiméticos derivados de la bestatina (KBE009)*

Compound	Structure	IC_{50} (µM)	highest $[I]_0/[E]_0$	% of inhibition
KBE009	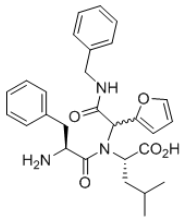	67.54 ± 4.02	1,333	60
KBE044	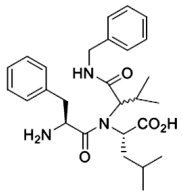	75.88 ± 2.80	2,666	80
KBE045	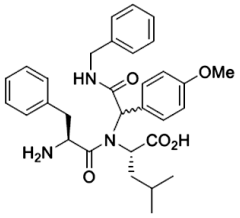	131.56 ± 16.27	5,333	60
KBE046	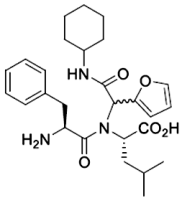	37.22 ± 3.82	5,333	90
KBE048	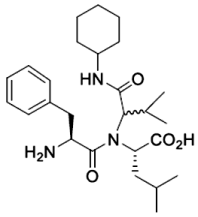	26.25 ± 4.99	5,333	80

The IC_{50} values are presented as mean ± standard error

Los valores de IC_{50} se presentan como la media ± el error estándar.

Table 1. Inhibition of the rePepN aminopeptidase by the bestatin (KBE009)-derived peptidomimetics-Continuation

Tabla 1. *Inhibición de la aminopeptidasa ePepNr por los peptidomiméticos derivados de la bestatina (KBE009)-Continuación*

Compound	Structure	IC_{50} (μM)	highest $[I]_0/[E]_0$	% of inhibition
KBE049	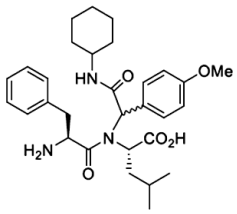	201.97 ± 19.38	5,333	60
KBE051	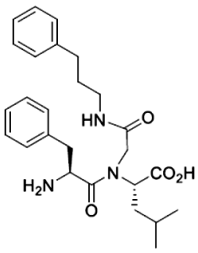	569.74 ± 107.57	10,666	60
KBE052	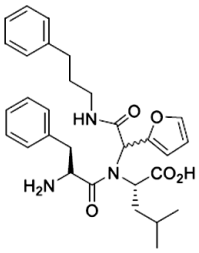	58.33 ± 9.06	1,333	60
KBE053	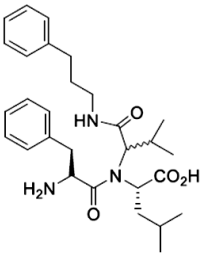	25.73 ± 2.26	1,333	80
KBE054	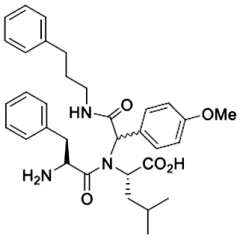	52.10 ± 8.09	1,333	70

The IC_{50} values are presented as mean ± standard error

Los valores de IC_{50} se presentan como la media ± el error estándar.

Once determined the IC_{50} values, the structure-activity relationship of these inhibitors was analyzed. For the compounds with a terminal benzyl or cyclohexyl group in the branch, the presence of the *p*-methoxyphenyl group at the center of the molecule significantly diminished the potency of the rePepN inhibition, comparing with the 2-furyl and isopropyl groups (table 1). The combination terminal cyclohexyl with central isopropyl generated one of the two most potent inhibitors in the library (KBE048, IC_{50} = 26 μM).

When the terminal group in the branch is 3-phenylpropyl, the absence of a central functional group notably increased the IC_{50} value, regarding the presence of the 2-furyl, isopropyl and *p*-methoxyphenyl groups (table 1). The first of these four cases corresponds to the worst inhibitor of the AP in this series (KBE051, IC_{50} = 570 µM), and the third resulted one of the two most potent inhibitors (KBE053, IC_{50} = 26 µM).

For the peptidomimetics with the central 2-furyl group, the most potent rePepN inhibition was obtained with the compound that has the terminal cyclohexyl group in the branch, in comparison with the benzyl and 3-phenylpropyl substituents (table 1). The same analysis for the inhibitors that have the central isopropyl group showed that the lowest IC_{50} values correspond to the molecules with the terminal cyclohexyl and 3-phenylpropyl groups. When the *p*-methoxyphenyl group occupies the central position, the decreasing order of the inhibitory activity corresponds to the peptidomimetics with the 3-phenylpropyl, benzyl and cyclohexyl functions at the end of the branch (table 1).

To determine the inhibition type of the bestatin (KBE009)-derived peptidomimetics toward the rePepN enzyme, the compound KBE053 was selected, since it is one of the two most potent in the series (IC_{50} = 26 µM). As it is shown in figure 4, this molecule is an uncompetitive inhibitor of the AP with a K_i = 10.13 µM.

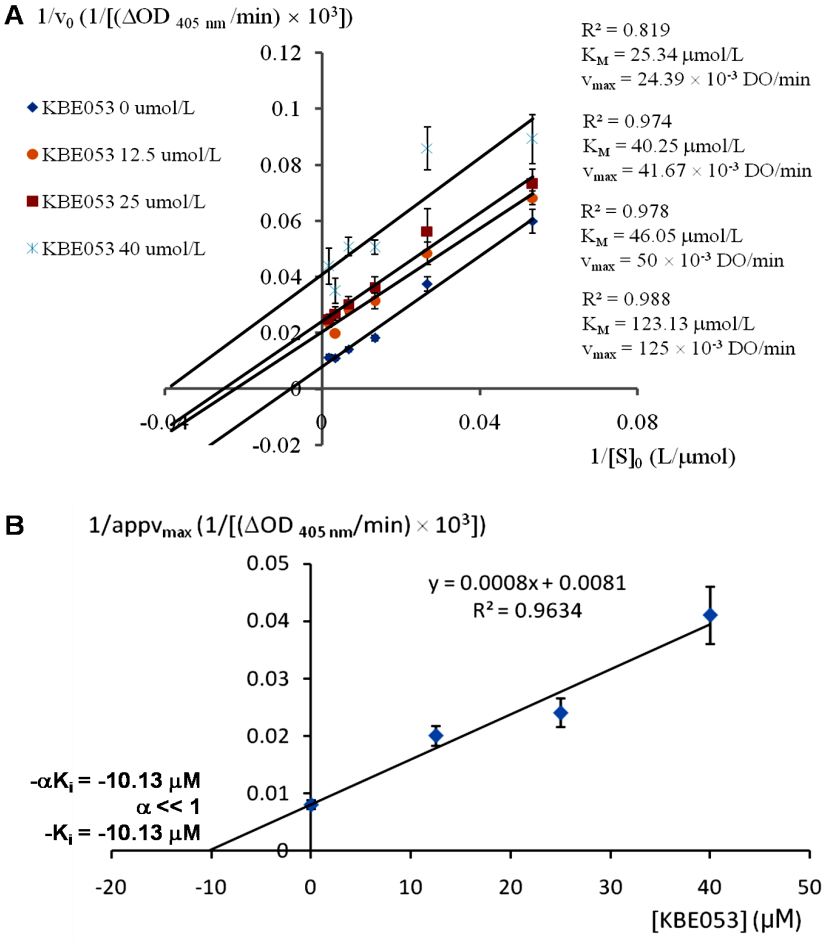

Figure 4. Some kinetic characteristics of ePepN inhibition by KBE053. A) Determination of the inhibition type. The K_M and maximum velocity (v_{max}) values are apparent. B) Dixon plot to determine the -K_i value (intercept with the abscise axis). Data are presented as mean ± standard deviation.

Figura 4. *Algunas características cinéticas de la inhibición de ePepN por KB053. A) Determinación del tipo de inhibición. Los valores de K_M y velocidad máxima ($v_{máx}$) son aparentes. B) Ploteo de Dixon para determinar el valor de -K_i (intercepto con el eje de las abscisas). Los datos se presentan como la media ± desviación estándar.*

The series of 10 synthetic bestatin (KBE009)-derived peptidomimetics was evaluated as possible rPfA-M1 inhibitors. This was performed in the same manner that for rePepN, carrying out dose-response studies and assessing the IC_{50} values. The 10 compounds resulted inhibitors of the AP, although showing different potency (table 2). The IC_{50} are extended between 13 and 423 µM, approximately. Similar to rePepN, three peptidomimetics have values higher than 100 µM (KBE045, 049 and 051), and seven in the 10-100 µM range (KBE009, 044, 046, 048, 052, 053 and 054).

Table 2. Inhibition of the rPfA-M1 aminopeptidase by the bestatin (KBE009)-derived peptidomimetics

Tabla 2. *Inhibición de la aminopeptidasa PfA-M1r por los peptidomiméticos derivados de la bestatina (KBE009)*

Compound	Structure	IC_{50} (µM)	highest $[I]_0/[E]_0$	% of inhibition
KBE009	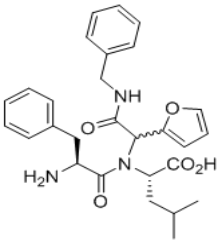	13.26 ± 2.49	1,887	70
KBE044	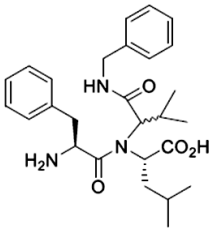	51.91 ± 2.56	3,774	70
KBE045	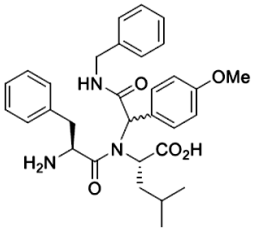	134.79 ± 1.30	5,660	80
KBE046	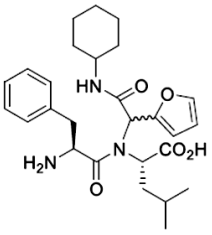	28.01 ± 3.56	2,830	70
KBE048	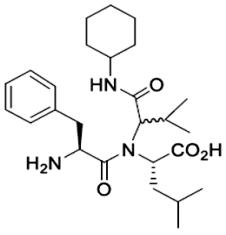	17.04 ± 1.41	1,887	70

The IC_{50} values are presented as mean ± standard error

Los valores de IC_{50} se presentan como la media ± el error estándar.

Table 2. Inhibition of the rPfA-M1 aminopeptidase by the bestatin (KBE009)-derived peptidomimetics-Continuation

Tabla 2. *Inhibición de la aminopeptidasa PfA-M1r por los peptidomiméticos derivados de la bestatina (KBE009)-Continuation*

Compound	Structure	IC_{50} (mM)	highest $[I]_0/[E]_0$	% of inhibition
KBE049	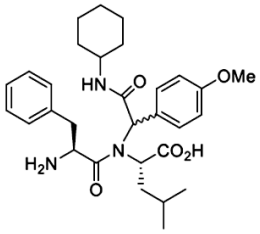	153.09 ± 1.17	5,660	70
KBE051	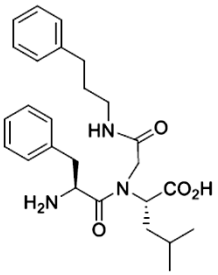	423.22 ± 31.15	15,094	75
KBE052	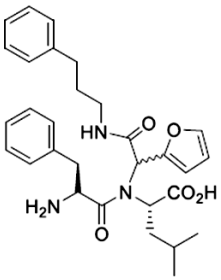	47.00 ± 4.92	3,774	75
KBE053	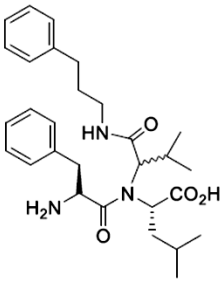	13.73 ± 2.96	1,887	75
KBE054	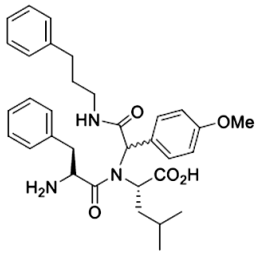	30.31 ± 5.18	3,774	75

The IC_{50} values are presented as mean ± standard error

Los valores de IC_{50} se presentan como la media ± el error estándar.

The determination of IC_{50} values allows to analyze the structure-activity relationship of these inhibitors. For the compounds with a terminal benzyl or cyclohexyl group in the branch, the presence of the central *p*-methoxyphenyl group also significantly diminished the potency of the rPfA-M1 inhibition, comparing with the 2-furyl and isopropyl groups (table 2). The combination terminal benzyl with central 2-furyl generated one of the two most potent inhibitors in the library (KBE009, IC_{50} = 13 µM). As occurred with rePepN, when the terminal group in the branch is 3-phenylpropyl, the absence of a central functional group notably increased the IC_{50} value, regarding the presence of the 2-furyl, isopropyl and *p*-methoxyphenyl groups (table 2). The first of these four cases corresponds to the worst rPfA-M1 inhibitor in this series (KBE051, IC_{50} = 423 µM), and the third resulted one of the two most potent inhibitors (KBE053, IC_{50} = 14 µM).

For the peptidomimetics with the central 2-furyl group, the most potent rPfA-M1 inhibition was obtained with the compound that has the terminal benzyl group in the branch, in comparison with the cyclohexyl and 3-phenylpropyl substituents (table 2). The same analysis for the inhibitors that have the central isopropyl group showed that, in the same manner that rePepN, the lowest IC_{50} values correspond to the molecules with the terminal cyclohexyl and 3-phenylpropyl groups. As occurred with rePepN, when the *p*-methoxyphenyl group occupies the central position, the decreasing order of the inhibitory activity corresponds to the peptidomimetics with the 3-phenylpropyl, benzyl and cyclohexyl terminal functions (table 2). Table 3 summarizes the structural determinants of these compounds for the inhibition of both APs.

Table 3. Structure-activity relationship for the inhibition of rePepN and rPfA-M1 aminopeptidases by the bestatin (KBE009)-derived peptidomimetics

Tabla 3. *Relación estructura-actividad para la inhibición de las aminopeptidasas ePepNr y PfA-M1r por los peptidomiméticos derivados de la bestatina (KBE009)*

Structural determinants for inhibition	rePepN	rPfA-M1
Common structural determinants for inhibition	central: isopropyl group terminal: 3-phenylpropyl group 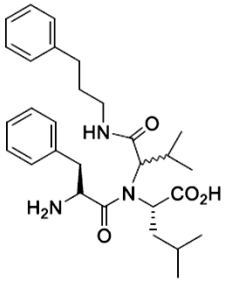 KBE053	
Different structural determinants for inhibition	central: isopropyl group terminal: cyclohexyl ring 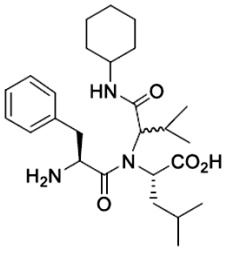 KBE048	central: 2-furyl group terminal: benzyl group 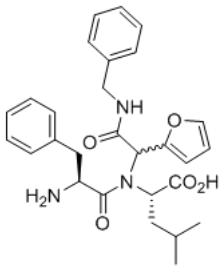 KBE009

DISCUSSION

The search for leading compounds for the development of drug candidates against human infectious diseases, caused by microorganisms, has become one of the worldwide priorities for biomedical research in the last years, due to the alarming increase of the microbial resistance to conventional antibiotics (Wilke, 2010; Silver, 2011; Pathak *et al*., 2012; Scholz *et al*., 2012; Dusano, 2016; Paterson, 2016). Among these efforts, the projects directed to identify protease inhibitors with potentialities as antimicrobial agents have a relevant place (Cathcart *et al*., 2011; Contreras-Martel *et al*., 2011; Newman *et al*., 2011; Turk *et al*., 2011; Singh *et al*., 2012; Zindel *et al*., 2013), since the crucial physiological functions of these enzymes for bacteria and fungi, and their relevance for pathogenesis (Kaman *et al*., 2014; Madigan *et al*., 2014). The neutral metallo-APs from various pathogen microorganisms are among the novel molecular targets recognized in the last decade, with possibilities to constitute the starting point of novel effective therapies (Florent *et al*., 1998; Cadavid-Restrepo *et al*., 2011; Drinkwater *et al*., 2017). For this reason, attempts to identify inhibitors of the microbial APNs, like ePepN, are highly relevant.

The enzyme PfA-M1, APN from *P. falciparum*, participates in the final stages of the human hemoglobin breakdown, process that occurs during the parasite erythrocytic stages (Gavigan *et al*., 2001; Dalal and Klemba, 2007; Harbut *et al*., 2011). Unlike the endoproteases that mediate the initial events of this essential process in the protozoon food vacuole (Liu *et al*., 2006), PfA-M1 is not functionally redundant with other APs produced by *P. falciparum* (Dalal and Klemba, 2007; Harbut *et al*., 2011; Skinner-Adams *et al*., 2012). The activity of this enzyme is considered indispensable for the erythrocytic development of the microorganism (Dalal and Klemba, 2007; Skinner-Adams *et al*., 2010). For these reasons, PfA-M1 is a promising target for the search for inhibitors with antimalarial activity (Harbut *et al*., 2011).

The identification of such compounds is of particular importance, due to the current prevalence of *P. falciparum* resistance to traditional drugs and the relevance of malaria as a global health, economic and social problem (WHO, 2017). Therefore, in the last years the search for inhibitors of this enzyme with potentialities as antimalarial drugs has been increased (Flipo *et al*., 2007a; Velmourougane *et al*., 2011; Mistry *et al*., 2014; Paiardini *et al*., 2015). With the exception of the non-selective inhibitor bestatin, from natural origin (Umezawa *et al*., 1976), all known PfA-M1 inhibitors, active against the parasite, are from synthetic origin (Flipo *et al*., 2007a; Skinner-Adams *et al*., 2007, 2012; Harbut *et al*., 2011; Velmourougane *et al*., 2011).

For the identification of enzymatic inhibitors, it is essential to first know the basic kinetic characteristics of the target enzyme, in order to adequately adjust the experimental conditions of the enzymatic assay. The equality between enzymatic activity values of the rePepN AP at pH 7.0 and 8.0 (Fig. 1A) is consistent with the selection of one or another pH value for other authors to perform the kinetic characterization studies of this enzyme (Chandu and Nandi, 2003; Chandu *et al.*, 2003; Golich *et al.*, 2006; Ito *et al.*, 2006; Kumar *et al.*, 2009). The same result was previously reported by Chappelet-Tordo and Lazdunski (1977) for the Ala-*p*NA substrate. Even when the optimal pH reported by Lazdunski *et al*. (1975) is 7.0, the result obtained in this work allowed to perform the enzymatic assay at pH 8.0. On the other hand, the appK_M value of 72 μM, obtained for rePepN with the Leu-*p*NA substrate (Fig. 1B), is lower than that recorded by Golich *et al*. (2006) of 200 ± 90 μM. This disparity could be the consequence of some little conformational difference between both recombinant variants of the AP.

The establishment of the inhibition equilibrium for the rePepN-bestatin couple, after a preincubation of 5 min (Fig. 2A), agrees with the observations of other authors that classify this compound as a slow-binding reversible inhibitor (Mucha *et al*., 2010). This means that minutes are required for establishing the equilibrium between the free enzyme and the inhibitor, on the one hand, and the enzyme-inhibitor complex, on the other. Although with these results it is not possible to classify the inhibitor as a fast- or slow-binding because experiments before 5 min were not performed. However, the non-competitive ($\alpha > 1$) or mixed character of the inhibition caused by bestatin (Fig. 2B) is not in agreement with the generally accepted classification of this pseudopeptide as a competitive inhibitor of metallo-APs, belonging to M1 and M17 families (Umezawa *et al*., 1976; Scornik and Botbol, 2001; Mucha *et al*., 2010). Such competitive effect for ePepN is not supported in the literature by kinetic studies at different substrate and bestatin

concentrations. For this reason, we decided to determine the inhibition mode of bestatin toward both enzymes, and taking into account that it is the parental compound of peptidomimetics. We had previously determined the IC_{50} of bestatin toward rePepN (7 µM; Méndez *et al*., 2019). The K_i = 2.31 µM (Fig. 2D) is consistent with the report of Fournié-Zaluski *et al.* (2009).

The establishment of the inhibition equilibrium for the rPfA-M1-bestatin, after a preincubation of 15 min (Fig. 3A), agrees with the reports of other authors that classify this compound as a slow-binding reversible inhibitor (Mucha *et al*., 2010). The K_i value of 1.29 µM determined in this work for bestatin toward rPfA-M1 (Fig. 3D) agrees with the reports of other authors that classify this compound as a micromolar-submicromolar inhibitor of the AP (Flipo *et al*., 2003, 2007a; McGowan *et al*., 2009; Ragheb *et al*., 2011; Skinner-Adams *et al*., 2012). This value is different than the K_i < 0.16 µM reported for bestatin toward this same enzyme, in the presence of Ala-7-amido-4-methylcoumarin (AMC) substrate (González-Bacerio *et al*., 2017). Apparently, the potency of an inhibitor toward the same enzyme could depend on the used substrate. Structural and size differences between the non-natural substrates Ala-AMC and Leu-*p*NA, and their dissimilar binding strength to the active site, could be responsible for the differential facility for substrate displacement by an inhibitor and, consequently, different inhibition potency.

The competitive inhibition caused by bestatin (Fig. 3C) agrees with the reports of other authors for M1- and M17-APs (Umezawa *et al*., 1976; Scornik and Botbol, 2001; Mucha *et al*., 2010). The relevance of this result (Fig. 3C) is that, to the best of our knowledge, such competitive effect for PfA-M1 is not based in the literature on kinetic studies at different substrate and bestatin concentrations. Despite the fact that PfA-M1 and ePepN share a 35 % total sequence identity (González-Bacerio *et al*., 2014b) and 85 % similarity in the active site region (Florent *et al*., 1998), bestatin inhibits both M1-APs with different inhibition modes (Fig. 2B and 3C). This could be due to subtle structural differences between both enzymes. At this respect, Pascual *et al*. (2017) also reported the non-competitive ($\alpha > 1$) or mixed inhibition of porcine APN (pAPN) by bestatin, even though some authors refer to bestatin as an APN competitive inhibitor (Wong *et al*., 2012).

What structural characteristics does PfA-M1 have in the active site that distinguish it from ePepN and pAPN and determine that the type of inhibition by bestatin is different? The enzyme PfA-M1 has a small active site that does not require a conformational change to bind ligands (McGowan *et al*., 2009). In ePepN, Met^{460} acts as a cushion to accommodate substrates and bestatin, altering the size of the active center (Addlagatta *et al*., 2006). The equivalent residue in rPfA-M1 is the smaller Val^{459}, which it is not displaced by the bestatin binding (McGowan *et al*., 2009). However, the ePepN active site is more flexible (there is evidence of domain movement), undergoing conformational changes between a closed (catalytically active) and open (substrate binding) form (Addlagatta *et al*., 2006). On the other hand, the pAPN active site is larger, allowing easy access to substrates (Chen *et al*., 2012). This is consistent with the physiological roles of this cell-surface ectoenzyme, which binds a wide range of peptides. This protein also experiments closed-open transitions, that allows it substrate binding, even exposed N-terminus of proteins (Chen *et al*., 2012). In addition, human APN does not bind bestatin in the same manner than substrate (Wong *et al*., 2012). The inhibitor is almost entirely covered by S1 subsite, coordinating the Zn^{2+} with the C-terminal carboxyl group. All these data suggest that bestatin can be accommodated in only one way in the PfA-M1 active site (competing with substrate), but the flexibility of the other proteins would allow the bestatin binding without competing with the substrate. This hypothesis would need confirmation.

In this work, enzymes titration was not possible, since an irreversible or tight-binding inhibitor is not available. However, although we cannot assure that all enzyme preparation is active, we can assure with a high probability (little variation) that proportion between active-inactive enzyme molecules will not change over time. A proof of this assumption is that we obtained similar results (IC_{50} values, the tendency is the same) with both enzymes (tables 1 and 2).

For the dose-response studies with the derived peptidomimetics a preincubation time of 15 min was used. This time was not determined for each compound. Instead, bestatin, the parental compound from which the others are derivatives, was used. Fifteen minutes is a prudent preincubation time to test compounds in an inhibition assay. Obtaining similar results (IC_{50} values) with both enzymes for each compound (tables 1 and 2) is evidence that there were no differences between them.

The inhibition of rePepN and rPfA-M1 by the 10 bestatin (KBE009)-derived peptidomimetics (tables 1 and 2) was an expected result, since the bestatin-derived peptidomimetic KBE009 inhibits rPfA-M1 (González-Bacerio *et al*., 2017), and other three bestatin-derived peptidomimetics (not presented here) also inhibit rePepN (Méndez *et al*., 2014). The weak or moderate inhibition of rePepN and rPfA-M1 by the 10 bestatin (KBE009)-derived peptidomimetics, described by IC_{50} values of hundreds to tens μM (tables 1 and 2), could be due to an inhibition mechanism that does not imply the coordination of the catalytic Zn^{2+} ion in the enzyme active site. We proposed this binding mode for the rPfA-M1-KBE009 complex, as a result of the application of an *in silico* molecular docking methodology (González-Bacerio *et al*., 2017). The absence of interactions with the Zn^{2+} could allow the inhibitor binding to the enzyme-substrate complex, to whose stabilization contribute the interactions between the metal cation and the substrate (Jones *et al*., 2011). This would be consistent with the uncompetitive inhibition observed in this work for the compound KBE053 toward rePepN (Fig. 4).

An important structural difference between the peptidomimetics tested in this work and bestatin, which coordinates the APNs catalytic Zn^{2+} in the enzyme-inhibitor complexes (Addlagatta *et al*., 2006; McGowan *et al*., 2009; Chen *et al*., 2012; Wong *et al*., 2012) and inhibits rePepN and rPfA-M1 with a K_i of units of mM (Fig. 2D and 3D), is the absence in the first of the a-hydroxyamide group, present in the bestatin's main chain. This is the inhibitor's chemical function that coordinates the Zn^{2+} in different AP-bestatin complexes, resolved by X-ray crystallography (Addlagatta *et al*., 2006; McGowan *et al*., 2009, 2010; Velmourougane *et al.*, 2011; Chen *et al*., 2012; Wong *et al*., 2012; Dalal *et al*., 2013).

Although none of the peptidomimetics in the library is a potent rePepN or rPfA-M1 inhibitor, their structural and IC_{50} variations contributed with valuable data for the study of the structure-activity relationship of these compounds toward the microbial APNs. The results of this analysis indicate that the presence of a central functional group, in the first carbon atom after the main chain's branch, is necessary to achieve the rePepN and rPfA-M1 inhibition with an IC_{50} of tens of μM (tables 1 and 2). However, apparently there is a size limit for this substituent, since the *p*-methoxyphenyl group is in general unfavorable in this position, comparing with the smaller 2-furyl and isopropyl (tables 1 and 2). The relevance of this substituent's volume increases when the size of the terminal group in the branch augments, since it tends to be more favorable for the inhibition the presence of the smallest of the tested central groups: the isopropyl (tables 1 and 2). This group combination (terminal 3-phenylpropyl in the branch and central isopropyl) generated one of the two most potent inhibitors in the series: the KBE053 (tables 1, 2 and 3). In this case, a displacement of the inhibitor in the complex with the enzyme could occur, with respects to the complexes with the compounds having smaller terminal groups in the branch, which could favor the hydrophobic interactions established by the small central isopropyl group.

Excluding the unfavorable central *p*-methoxyphenyl group, together with the other tested central substituents, the greater flexibility of the terminal cyclohexyl ring in the branching seems to be important for the inhibition (tables 1 and 2). It should be emphasized that the combination of the terminal cyclohexyl group in the branch and central isopropyl generated the other of the two most potent rePepN inhibitors in the series: the KBE048 (tables 1 and 3). However, for rPfA -M1, the combination of the terminal benzyl group in the branch and central 2-furyl generated the other of the two most potent inhibitors in the series: the KBE009 (tables 2 and 3). This divergence between both M1-APs could be caused by the previously mentioned subtle structural difference. As occurs with bestatin, the K_i of KBE009 toward rPfA-M1 in the presence of Ala-AMC substrate is submicromolar (0.4 μM; González-Bacerio *et al*., 2017). In this work, the IC_{50} of KBE009 against the same enzyme in the presence of Leu-*p*NA substrate was 13 μM (table 2). This disparity could be due to the previously mentioned structural and size differences between both artificial substrates.

These results are in agreement with the previous docking predictions for the rPfA-M1-KBE009 complex (González-Bacerio *et al*., 2017). According to this model, the terminal benzyl group in the branch of KBE009 interacts hydrophobically with the side chains of several residues in the S1 pocket of the rPfA-M1 active site. Taking into account the flexibility of this pocket (Velmourougane *et al*., 2011), the terminal 3-phenylpropyl or cyclohexyl groups can also be accommodated on this site of both APs. In addition, this

model predicts that the 2-furyl group of KBE009 is placed between the S1 and S1' subsites, interacting hydrophobically with V^{459} of rPfA-M1 (González-Bacerio *et al*., 2017). Such prediction is consistent with the favorable interactions of the little isobutyl group in the small space between the S1 and S1' subsites.

The knowledge of the kinetic type of inhibition of a target enzyme by a family of structurally related compounds is of crucial relevance to elucidate the mechanism of inhibition and to guide the optimization of the molecule central backbone, with the aim to increase the potency and selectivity of the inhibitory activity (Flipo *et al*., 2007b). It also facilitates the *in silico* studies of the binding mode of the inhibitor to the enzyme and contributes to the design of novel inhibitors, in function of the desired application (Flipo *et al*., 2003, 2007a). In the case of ePepN AP, not kinetic studies are found in the literature aimed at determining the inhibition type of compounds with inhibitory activity of this enzyme. Therefore, the determination in this work of the rePepN inhibition in an uncompetitive mode, by the KBE053 peptidomimetic (Fig. 4), is a relevant contribution to the body of knowledge in this field. The inhibition type of rPfA-M1 by KBE053 was not assessed by availability issues.

In conclusion, the EA of rePepN AP at pH 7.0 and 8.0, and the obtained appK_M value, indicate that the recombinant enzyme is a good model of the natural one for the inhibitors identification. Bestatin is a non-competitive ($\alpha > 1$) or mixed inhibitor of rePepN, with a K_i = 2.31 μM, which means that it is possible to achieve potent inhibition of this APN by this type of inhibition. On the other hand, bestatin is a slow-binding competitive inhibitor of the rPfA-M1 enzyme, with a K_i = 1.29 μM. This can be extrapolated to the development of other inhibitors.

The structural characteristics of the synthetic bestatin (KBE009)-derived peptidomimetics that are favorable for the inhibition of rePepN and rPfA-M1 are: the presence in the branch of the little central isopropyl group and the terminal 3-phenylpropyl group. For rePepN, another successful combination is the central isopropyl group and the terminal flexible cyclohexyl ring. However, for rPfA-M1, the other most potent inhibitory combination is the central 2-furyl and terminal benzyl groups.

The type of inhibition of the KBE053 peptidomimetic, as representative of this compound series, is uncompetitive toward rePepN with a K_i = 10.13 μM. This knowledge could facilitate the *in silico* study of the binding mode of inhibitors to the enzyme, guide the future optimization of these structures and contribute to the design of novel rePepN inhibitors.

ACKNOWLEDGEMENTS

This work was supported by the International Foundation for Sciences (grant F/4730-2), and the project assigned to J. González-Bacerio and associated to the Cuban National Program of Basic Sciences.

CITED LITERATURE

Addlagatta, A., L. Gay and B.W. Matthews (2006) Structure of aminopeptidase N from *Escherichia coli* suggests a compartmentalized, gated active site. Proc. Natl. Acad. Sci. USA 103(36): 13339-13344.

Addlagatta, A., L. Gay and B.W. Matthews (2008) Structural basis for the unusual specificity of *Escherichia coli* aminopeptidase N. Biochemistry 47(19): 5301-5311.

Albiston, A.L., S. Ye and S.Y. Chai (2004) Membrane bound members of the M1 family: more than aminopeptidases. Protein Pept. Lett. 11(5): 491-500.

Allary, M., J. Schrével and I. Florent (2002) Properties, stage-dependent expression and localization of *Plasmodium falciparum* M1 family zinc-aminopeptidase. Parasitology 125: 1-10.

Azimzadeh, O., C. Sow, M. Gèze, J. Nyalwidhe *et al*. (2010) *Plasmodium falciparum* PfA-M1 aminopeptidase is trafficked via the parasitophorous vacuole and marginally delivered to the food vacuole. Malaria J. 9: 189-204.

Barret, A.J., N.M. Rawlings and J.F. Woessner (2003) Introduction: metallopeptidases and their clans. In: Barret, A.J., N.M. Rawlings and J.F. Woessner (Eds.), Handbook of proteolytic enzymes, 2nd Edition. Academic Press, London. pp. 334-542.

Burley, S.K., P.R. David and W.N. Lipscomb (1991) Leucine aminopeptidase: bestatin inhibition and a model for enzyme-catalyzed peptide hydrolysis. Proc. Natl. Acad. Sci. USA 88 (16): 6916-6920.

Cadavid-Restrepo, G., T.S. Gastardelo, E. Faudry, H. de Almeida *et al*. (2011) The major leucyl aminopeptidase of *Trypanosoma cruzi* (LAPTc) assembles into a homohexamer and belongs to the M17 family of metallopeptidases. BMC Biochem. 12: 46-59.

Cathcart, G., D. Quinn and B. Greer (2011) Novel inhibitors of the *Pseudomonas aeruginosa* virulence factor LasB: a potential therapeutic approach for the attenuation of virulence mechanisms in pseudomonal infection. Antimicrob. Agents Chemother. 55: 2670-2678.

Chandu, D. and D. Nandi (2003) PepN is the major aminopeptidase in *Escherichia coli*: insights on substrate specificity and role during sodium-salicylate-induced stress. Microbiology 149: 3437-3447.

Chandu, D., A. Kumar and D. Nandi (2003) PepN, the major Suc-LLVY-AMC-hydrolyzing enzyme in *Escherichia coli*, displays functional similarity with downstream processing enzymes in Archaea and Eukarya. J. Biol. Chem. 278: 5548-5556.

Chappelet-Tordo, D. and C. Lazdunski (1977) Aminopeptidase N from *Escherichia coli*: ionizable active-center groups and substrate specificity. J. Biochem. 81: 299-305.

Chen, L., Y-L. Lin, G. Peng and F. Li (2012) Structural basis for multifunctional roles of mammalian aminopeptidase N. Proc. Natl. Acad. Sci. USA 109(44): 17966-17971.

Contreras-Martel, C., A. Amoroso and E. Woon (2011) Structure guided design of cell wall biosynthesis inhibitors that overcome betalactam resistance in *Staphylococcus aureus* (MRSA). ACS Chem. Biol. 6: 943-951.

Copeland, R.A. (2000) Enzymes: A practical introduction to structure, mechanism, and data analysis. 2nd Edition. Wiley-VCH, Inc., New York.

Dalal, S. and M. Klemba (2007) Roles for two aminopeptidases in vacuolar hemoglobin catabolism in *Plasmodium falciparum*. J. Biol. Chem. 282(49): 35978-35987.

Dalal, S., D.R.T. Ragheb and M. Klemba (2012) Engagement of the S1, S1' and S2' subsites drives efficient catalysis of peptide bond hydrolysis by the M1-family aminopeptidase from *Plasmodium falciparum*. Mol. Biochem. Parasitol. 183: 70-77.

Dalal, S., D.R.T. Ragheb, F.D. Schubot and M. Klemba (2013) A naturally variable residue in the S1 subsite of M1 family aminopeptidases modulates catalytic properties and promotes functional specialization. J. Biol. Chem. 288: 26004-26012.

Dong, L., N. Cheng, M. Wang, J. Zhang *et al*. (2005) The leucyl aminopeptidase from *Helicobacter pylori* is an allosteric enzyme. Microbiology 151: 2017-2023.

Doolan, D.L., S.H. Apte and C. Proietti (2014) Genome-based vaccine design: the promise for malaria and other infectious diseases. Int. J. Parasitol. 44(12): 901-913.

Drinkwater, N., J. Lee, W. Yang, T.S. Malcolm *et al*. (2017) M1 aminopeptidases as drug targets: Broad applications or therapeutic niche? FEBS J. 284(10): 1473-1488.

Drinkwater, N., R.S. Bamert, K. Kannan Sivaraman, A. Paiardini *et al.* (2015) X-ray crystal structures of an orally available aminopeptidase inhibitor, Tosedostat, bound to anti-malarial drug targets PfA-M1 and PfA-M17. Proteins 83(4): 789-795.

Dusano, G. (2016) Antibacterial chemotherapy. In: Goldman, L. and A.I. Schafer (Eds.), Goldman-Cecil Med, 25th Edition. Elsevier, Canada. pp. 1885-1896.

Flipo, M., I. Florent, P. Grellier, C. Sergheraerta *et al*. (2003) Design, synthesis and antimalarial activity of novel, quinoline-based, zinc metallo-aminopeptidase inhibitors. Bioorg. Med. Chem. Lett. 13(16): 2659-2662.

Flipo, M., T. Beghyn, J. Charton, V. Leroux *et al*. (2007b) A library of novel hydroxamic acids targeting the metalloprotease family: design, parallel synthesis and screening. Bioorg. Med. Chem. 15: 63-76.

Flipo, M., T. Beghyn, V. Leroux, I. Florent *et al*. (2007a) Novel selective inhibitors of the zinc plasmodial aminopeptidase PfA-M1 as potential antimalarial agents. J. Med. Chem. 50 (6): 1322-1334.

Florent, I., Z. Derhy, M. Allary, M. Monsigny *et al*. (1998) A *Plasmodium falciparum* aminopeptidase gene belonging to the M1 family of zinc-metallopeptidases is expressed in erythrocytic stages. Mol. Biochem. Parasitol. 97: 149-160.

Fournié-Zaluski, M.C., H. Poras, B.P. Roques, Y. Nakajima *et al*. (2009) Structure of aminopeptidase N from *Escherichia coli* complexed with the transition-state analogue aminophosphinic inhibitor PL250. Acta Cryst. D65: 814-822.

Gavigan, C.S., J.P. Dalton and A. Bell (2001) The role of aminopeptidases in haemoglobin degradation in *Plasmodium falciparum*-infected erythrocytes. Mol. Biochem. Parasitol. 117: 37-48.

Golich, F., M. Han and M. Crowder (2006) Over-expression, purification, and characterization of aminopeptidase N from *Escherichia coli*. Protein Expr. Purif. 47: 634-639.

González-Bacerio, J., J. Osuna, A. Ponce, R. Fando *et al*. (2014a) High-level expression in *Escherichia coli*, purification and kinetic characterization of *Plasmodium falciparum* M1-aminopeptidase. Protein Expr. Purif. 104: 103-114.

González-Bacerio, J., R. Fando, A. del Monte-Martínez, J-L. Charli *et al*. (2014b) *Plasmodium falciparum* M1-aminopeptidase: A promising target for the development of antimalarials. Curr. Drug Targets 15: 1144-1165.

González-Bacerio, J., S.E.C. Maluf, Y. Méndez, I. Pascual *et al*. (2017) KBE009: An antimalarial bestatin-like inhibitor of the *Plasmodium falciparum* M1 aminopeptidase discovered in an Ugi multicomponent reaction-derived peptidomimetic library. Bioorg. Med. Chem. 25(17): 4628-4636.

Greenwood, B.M., K. Bojang, C.J. Whitty and G.A. Targett (2005) Malaria. Lancet 365(9469): 1487-1498.

Harbut, M.B., G. Velmourougane, S. Dalal, G. Reissa *et al*. (2011) Bestatin-based chemical biology strategy reveals distinct roles for malaria M1- and M17-family aminopeptidases. Proc. Natl. Acad. Sci. USA 108(34): E526-E534.

Ito, K., Y. Nakajima, Y. Onohara, M. Takeo *et al*. (2006) Crystal structure of aminopeptidase N (proteobacteria alanyl aminopeptidase) from *Escherichia coli* and conformational change of methionine 260 involved in substrate recognition. J. Biol. Chem. 281: 33664-33676.

Jones, P.M., M.W. Robinson, J.P. Dalton and A.M. George (2011) The *Plasmodium falciparum* malaria M1 alanyl aminopeptidase (PfA-M1): Insights of catalytic mechanism and function from MD simulations. PLoS One 6(12): e28589.

Kaman, W., J. Hays, H. Endtz and F. Bikker (2014) Bacterial proteases: targets for diagnostics and therapy. Eur. J. Clin. Microbiol. Infect. Dis. 33: 1081-1087.

Kannan Sivaraman, K., A. Paiardini, M. Sieńczyk, C. Ruggeri *et al.* (2013) Synthesis and structure-activity relationships of phosphonic arginine mimetics as inhibitors of the M1 and M17 aminopeptidases from *Plasmodium falciparum*. J. Med. Chem. 56(12): 5213-5217.

Kumar, A., M. Bhosale, S. Reddy, N. Srinivasan *et al*. (2009) Importance of non-conserved distal carboxyl terminal amino acids in two peptidases belonging to the M1 family: *Thermoplasma acidophilum* Tricorn interacting factor F2 and *Escherichia coli* peptidase N. Biochimie 91: 1145-1155.

Labbé, S., D. Grenier, P. Plamondon, V-J. Uitto *et al*. (2001) Effects of dipeptide bestatin on *Porphyromonas gingivalis* and epithelial cells. J. Periodontol. 72(6): 714-721.

Lazdunski, C., J. Busuttil and A. Lazdunski (1975) Purification and properties of a periplasmic aminoendopeptidase from *Escherichia coli*. Eur. J. Biochem. 60: 363-369.

Liu, J., E.S. Istvan, I.Y. Gluzman, J. Gross *et al*. (2006) *Plasmodium falciparum* ensures its amino acid supply with multiple acquisition pathways and redundant proteolytic enzyme systems. Proc. Natl. Acad. Sci. USA 103(23): 8840-8845.

Luan, Y. and W. Xu (2007) The structure and main functions of aminopeptidase N. Curr. Med. Chem. 14(6): 639-647.

Madigan, M., J. Martinko, K. Bender, D. Buckley *et al*. (2014) Brock biology of microorganisms. 14th Edition. Pearson Education, Inc., USA.

McGowan, S., C.A. Oellig, W.A. Birru, T.T. Caradoc-Davies *et al*. (2010) Structure of the *Plasmodium falciparum* M17 aminopeptidase and significance for the design of drugs targeting the neutral exopeptidases. Proc. Natl. Acad. Sci. USA 107(6): 2449-2454.

McGowan, S., C.J. Porter, J. Lowther, C.M. Stack *et al*. (2009) Structural basis for the inhibition of the essential *Plasmodium falciparum* M1 neutral aminopeptidase. Proc. Natl. Acad. Sci. USA 106(8): 2537-2542.

Méndez, Y., G. De Armas, I. Pérez, T. Rojas *et al*. (2019) Discovery of potent and selective inhibitors of the *Escherichia coli* M1-aminopeptidase via multicomponent solid-phase synthesis of tetrazole-peptidomimetics. Eur. J. Med. Chem. 163: 481-499.

Méndez, Y., K. Pérez-Labrada, J. González-Bacerio, G. Valdés *et al*. (2014) Combinatorial multicomponent access to natural-products-inspired peptidomimetics: Discovery of selective inhibitors of microbial metallo-aminopeptidases. ChemMedChem 9: 2351-2359.

Mistry, S.N., N. Drinkwater, C. Ruggeri, K. Kannan Sivaraman *et al*. (2014) Two-pronged attack: Dual inhibition of *Plasmodium falciparum* M1 and M17 metalloaminopeptidases by a novel series of hydroxamic acid-based inhibitors. J. Med. Chem. 57(21): 9168-9183.

Modak, J., W. Rut, L. Wijeyewickrema, R. Pike *et al*. (2016) Structural basis for substrate specificity of *Helicobacter pylori* M17 aminopeptidase. Biochimie 121: 60-71.

Morty, R.E. and J. Morehead (2002) Cloning and characterization of a leucyl aminopeptidase from three pathogenic *Leishmania* species. J. Biol. Chem. 277(29): 26057-26065.

Mucha, A., M. Drag, J. Dalton and P. Kafarski (2010) Metalloaminopeptidase inhibitors. Biochimie 92: 1509-1529.

Nankya-Kitaka, M., G. Curley, C. Gavigan, A. Bell *et al*. (1998) *Plasmodium chabaudi chabaudi* and *P. falciparum*: Inhibition of aminopeptidase and parasite growth by bestatin and nitrobestatin. Parasitol. Res. 84(7): 552-558.

Newman, Z., N. Sirianni and C. Mawhinney (2011) Auranofin protects against anthrax lethal toxin-induced activation of the Nlrp1b inflammasome. Antimicrob. Agents Chemother. 55: 1028-1035.

Noble, F. and B.P. Roques (2007) Protection of endogenous enkephalin catabolism as natural approach to novel analgesic and antidepressant drugs. Expert Opin. Ther. Targets 11 (2): 145-159.

Omara-Opyene, A.L., P.A. Moura, C.R. Sulsona, J.A. Bonilla *et al*. (2004) Genetic disruption of the *Plasmodium falciparum* digestive vacuole plasmepsins demonstrates their functional redundancy. J. Biol. Chem. 279(52): 54088-54096.

Paiardini, A., R.S. Bamert, K. Kannan Sivaraman, N. Drinkwater *et al*. (2015) Screening the medicines for Malaria Venture "Malaria Box" against the *Plasmodium falciparum* aminopeptidases, M1, M17 and M18. PLoS One 10(2): e0115859.

Pascual, I., P.A. Valiente, G. García, M.E. Valdés-Tresanco *et al*. (2017) Discovery of novel non-competitive inhibitors of mammalian neutral M1 aminopeptidase (APN). Biochimie 142: 216-225.

Paterson, D. (2016) Infections due to other members of the Enterobacteriaceae, including management of multidrug-resistant strains. In: Goldman, L. and A.I. Schafer (Eds.), Goldman-Cecil Med, 25th Edition. Elsevier, Canada. pp. 1960-1962.

Pathak, A., Y. Marothi, V. Kekre, K. Mahadik *et al*. (2012) High prevalence of extended spectrum b-lactamase-producing pathogens results of a surveillance study in two hospitals in Ujjain, India. Infect. Drug Resist. 5: 65-73.

Poreba, M., S. McGowan, T.S. Skinner-Adams, K.R. Trenholme *et al*. (2012) Fingerprinting the substrate specificity of M1 and M17 aminopeptidases of human malaria, *Plasmodium falciparum*. PLoS One 7(2): e31938.

Ragheb, D., S. Dalal, K.M. Bompiani, W.K. Ray *et al*. (2011) Distribution and biochemical properties of an M1-family aminopeptidase in *Plasmodium falciparum* indicate a role in vacuolar hemoglobin catabolism. J. Biol. Chem. 286(31): 27255-27265.

Rosati, M., S. Dalal and M. Klemba (2017) Two cap residues in the S1 subsite of a *Plasmodium falciparum* M1-family aminopeptidase promote broad specificity and enhance catalysis. Mol. Biochem. Parasitol. 217: 7-12.

Scholz, T., C. Heyl, D. Bernardi, S. Zimmermmann *et al*. (2012) Chemical, biochemical and microbiological properties of a brominated nitrovinylfuran with broad-spectrum antibacterial activity. Bioorg. Med. Chem. 21: 795-804.

Scornik, O. and V. Botbol (2001) Bestatin as an experimental tool in mammals. Curr. Drug Metab. 2: 67-85.

Silver, L.L. (2011) Challenges of antibacterial discovery. Clin. Microbiol. Rev. 24(1): 71-109.

Singh, S.K., L. SaiSree, R.N. Amrutha and M. Reddy (2012) Three redundant murein endopeptidases catalyse an essential cleavage step in peptidoglycan synthesis of *Escherichia coli* K12. Mol. Microbiol. 86(5): 1036-1051.

Skinner-Adams, T.S., C.L. Peatey, K. Anderson, K.R. Trenholme *et al*. (2012) The aminopeptidase inhibitor CHR-2863 is an orally bioavailable inhibitor of murine malaria. Antimicrob. Agents Chemother. 56(6): 3244-3249.

Skinner-Adams, T.S., C.M. Stack, K.R. Trenholme, C.L. Brown *et al*. (2010) *Plasmodium falciparum* neutral aminopeptidases: New targets for anti-malarials. Trends Biochem. Sci. 35: 53-61.

Skinner-Adams, T.S., J. Lowther, F. Teuscher, C.M. Stack *et al*. (2007) Identification of phosphinate dipeptide analog inhibitors directed against the *Plasmodium falciparum* M17 leucine aminopeptidase as lead antimalarial compounds. J. Med. Chem. 50(24): 6024-6031.

Snedecor, G.W. and W.G. Cochran (1989) Statistical methods. 8th Edition. Iowa State University Press, Iowa.

Tieku, S. and N.M. Hooper (1992) Inhibition of aminopeptidases N, A and W: A reevaluation of the action of bestatin and inhibitors of angiotensin converting enzyme. Biochem. Pharmacol. 44: 1725-1730.

Tukey J. (1949) Comparing individual means in the analysis of variance. Biometrics 5: 99-114.

Turk, S., O. Verlaine, T. Gerards and M. Zivec (2011) New noncovalent inhibitors of penicillin-binding proteins from penicillin-resistant bacteria. PLoS One 6(5): e19418.

Turschner, S. and T. Efferth (2009) Drug resistance in *Plasmodium*: Natural products in the fight against malaria. Mini-Rev. Med. Chem. 9(2): 1-9.

Umezawa, H., T. Aoyagi, H. Suda, M. Hamada *et al*. (1976) Bestatin, an inhibitor of aminopeptidase B, produced by actinomycetes. J. Antibiot. (Tokyo) 29(1): 97-99.

Velmourougane, G., M.B. Harbut, S. Dalal, S. McGowan *et al*. (2011) Synthesis of new (-)-bestatin-based inhibitor libraries reveals a novel binding mode in the S1 pocket of the essential malaria M1 metalloaminopeptidase. J. Med. Chem. 54: 1655-1666.

Wilke, M.H. (2010) Multiresistant bacteria and current therapy - the economical side of the story. Eur. J. Med. Res. 15(12): 571-576.

Wong, A., D. Zhou and J. Rini (2012) The X-ray crystal structure of human aminopeptidase N reveals a novel dimer and the basis for peptide processing. J. Biol. Chem. 287(44): 36804-36813.

World Health Organization (WHO) (2017). World Malaria Report 2017. Available in: http://www.who.int/malaria/publications/world-malaria-report-2017/en/ [access: June 4th 2018].

Xu, W. and Q. Li (2005) Pogress in the development of aminopeptidase N (APN/CD13) inhibitors. Curr. Med. Chem. 5: 281-301.

Yeh, I. and R.B. Altman (2006) Drug targets for *Plasmodium falciparum*: A post-genomic review/survey. Mini-Rev. Med. Chem. 6: 177-202.

Zindel, S., W. Kaman and S. Fröls (2013) The papain inhibitor (SPI) of *Streptomyces mobaraensis* inhibits bacterial cysteine proteases and is an antagonist of bacterial growth. Antimicrob. Agents Chemother. 57: 3388-3391.